

# Antibacterial activity of gold nanorods against *Staphylococcus aureus* and *Propionibacterium acnes*: misinterpretations and artifacts

Nouf N Mahmoud  
Alaaldin M Alkilany  
Enam A Khalil  
Amal G Al-Bakri

Department of Pharmaceutics and  
Pharmaceutical Technology, School  
of Pharmacy, The University of Jordan,  
Amman, Jordan

**Abstract:** The antibacterial activity of gold nanorod (GNR) suspensions of different surface functionalities was investigated against standard strains of *Staphylococcus aureus* and *Propionibacterium acnes*, taking into consideration two commonly “overlooked” factors: the colloidal stability of GNR suspensions upon mixing with bacterial growth media and the possible contribution of “impurities/molecules” in GNR suspensions to the observed antibacterial activity. The results demonstrated that cationic polyallylamine hydrochloride (PAH)-GNR were severely aggregated when exposed to bacterial growth media compared to other GNR suspensions. In addition, the free cetyltrimethylammonium bromide (CTAB) present in GNR suspensions is most likely the origin of the observed antibacterial activity. However, the antibacterial activity of GNR themselves could not be excluded. Probing these two critical control studies prevents misinterpretations and artifacts of the antibacterial activity of nanoparticles. Unfortunately, these practices are usually ignored in the published studies and may explain the significant conflicting results. In addition, this study indicates that GNR could be a promising candidate for the treatment of skin follicular diseases such as acne vulgaris.

**Keywords:** antibacterial activity, supernatant, gold nanorods, colloidal stability, artifacts, acne vulgaris

## Introduction

Gold nanoparticles (GNP) with non-spherical shape, such as gold nanorods (GNR), are gaining particular attention as antimicrobial candidate. In addition to their biocompatibility and ease of functionalization, they extensively absorb near infra-red (NIR) light that is within an appropriate wavelength window for therapeutic applications,<sup>1,2</sup> resulting in local hyperthermia that can be used to eliminate microorganisms.<sup>3-5</sup> Large body of research has been conducted to explore the antibacterial activity of GNP of different shapes and physiochemical properties toward different bacterial strains, nevertheless the findings are conflicting.<sup>6-11</sup>

Acne vulgaris is a chronic skin inflammatory disease; it results in comedones or severe inflammatory lesions in the face, back, and chest. The pathophysiology of acne includes abnormal proliferation and differentiation of keratinocytes, increased sebum production, and hyperproliferation of microorganisms that are part of the normal skin flora, mainly *Propionibacterium acnes*, *Staphylococcus aureus*, and *S. epidermidis*.<sup>12,13</sup> Most of the conventional available therapeutic agents for acne are usually associated with severe side effects and high cost in addition to bacterial resistance that diminish the patient compliance. GNP have several advantages in skin and follicular drug

Correspondence: Amal G Al-Bakri  
Department of Pharmaceutics and  
Pharmaceutical Technology, School of  
Pharmacy, The University of Jordan,  
Amman 11942, Jordan  
Tel +962 6 535 5000 ext 23330  
Fax +962 6 530 0250  
Email agbakri@ju.edu.jo

delivery;<sup>14–16</sup> however, the potential antimicrobial activity of GNR against microorganisms commonly responsible for skin and follicular diseases was rarely investigated.

Despite the attractive properties of GNR, they have a high tendency to aggregate especially in the presence of high salts and biomolecules.<sup>17,18</sup> The colloidal stability of GNP in biological fluids is essential in most applications, such as drug delivery, imaging, and diagnosis. Bacterial growth media (for in vitro studies) are rich in peptides, amino acids, electrolytes, and other chemicals, which may induce aggregation of nanoparticles. Despite the increasing interest in understanding the fate of nanomaterials in biological media,<sup>19–21</sup> to the best of our knowledge, no systematic investigations on the colloidal stability of GNR when mixed with bacterial growth media were conducted in the literature. Ignoring such a critical factor will ultimately lead to serious misinterpretations of the results and outcomes. Similarly, the toxic effect of free molecules and impurities such as cetyltrimethylammonium bromide (CTAB) on bacterial culture was not previously evaluated in the studies which explored the antibacterial activity of GNR prepared using CTAB.

Herein, the antibacterial activity of GNR of different surface chemistry was investigated against *S. aureus* and *P. acnes*, which contribute to the pathogenesis of acne vulgaris. In addition, two critical controls were systematically investigated while measuring the antibacterial activity of GNR; first, the colloidal stability of GNR suspensions of different surface chemistry upon mixing with the bacterial growth media. Second, the antibacterial activity of the supernatants and the extra-purified GNR suspensions compared to the original GNR suspensions.

## Materials and instrumentations

The following materials were obtained from Sigma Aldrich Co., St Louis, MO, USA: chloroauric acid ( $\text{HAuCl}_4 \cdot 3\text{H}_2\text{O}$ , 99.9%), sodium borohydride ( $\text{NaBH}_4$ , 99%), silver nitrate ( $\text{AgNO}_3$ , 99%), ascorbic acid (99%), polyallylamine hydrochloride (PAH, MW ~15,000 g/mole), polyacrylic acid (PAA, sodium salt, MW ~15,000 g/mole), methoxy polyethylene glycol thiol (m-PEG-SH, MW ~2,000 g/mole), CTAB (99%), sodium chloride (NaCl), poly-L-lysine solution, and epoxy embedding medium kit.

Cystamine dihydrochloride (97%) was obtained from Acros, UK. Glutaraldehyde (25%) was obtained from Koch-Light Laboratories Ltd., UK. Formvar-coated copper transmission electron microscope (TEM) grids (300 meshes) were obtained from Ted Pella Inc., Canada. Ninety-six-well

plates and 24-well plates were obtained from Greiner bio-one, Germany.

Nutrient broth, reinforced clostridial broth, agar bacteriological (agar no 1), nutrient agar, Mueller–Hinton broth, *S. aureus* ATCC 29213, and *P. acnes* ATCC 11827 were obtained from Oxoid, UK.  $\text{CO}_2$  generator sachets (15%) were obtained from Thermo Fisher Scientific, Waltham, MA, USA.

Ultraviolet–visible (UV-vis) absorption spectra of GNR were determined using UV-vis spectrophotometer (Spectrascan 80D, Biotech Eng., UK) over the range of 400–1,100 nm. TEM images and scanning electron microscope (SEM) images were obtained using Versa 3D, FEI, Holland, operating at 30 kV. Dynamic light scattering (DLS) and zeta potential analysis were performed using Microtrac Zetatrak, Betatek Inc., Canada. Centrifugation of suspensions was performed using Centrifuge Z 216 M, Hermle Labortechnik, Germany.

All chemicals were used as received from suppliers, and all solutions used in preparation of GNP were prepared with purified 18 M $\Omega$  water. All glassware were cleaned with aqua regia thoroughly and rinsed with purified 18 M $\Omega$  water before use.

## Methods

### Synthesis of CTAB-capped GNR (CTAB-GNR)

CTAB-GNR were synthesized according to the seed-mediated surfactant-assisted wet-chemical method.<sup>22</sup> For the seed synthesis, a solution of 0.25 mM  $\text{HAuCl}_4$  was prepared in 0.1 M CTAB.  $\text{NaBH}_4$  (0.6 mL, 10 mM) was added to 10 mL of gold-CTAB solution with stirring. For GNR synthesis, the following agents were added to the CTAB aqueous solution (95 mL, 0.1 M) with gentle mixing:  $\text{AgNO}_3$  solution (1.1 mL, 10 mM) to get GNR with aspect ratio (AR; length/width) of ~4,  $\text{HAuCl}_4$  solution (5 mL, 10 mM), ascorbic acid solution (0.55 mL, 0.1 M), and finally seed solution (0.12 mL). GNR mixture left undisturbed at 25°C overnight. To get rid of the excess CTAB, GNR suspension was centrifuged twice for 15 min at 12,000 rpm, and the pellets were resuspended in purified 18 M $\Omega$  water.

### PAA coating of CTAB-GNR

To each 1.0 mL of twice purified CTAB-GNR suspension, 0.2 mL of PAA solution (10 mg/mL prepared in 10 mM NaCl solution) and 0.1 mL NaCl solution (10 mM) were added simultaneously.<sup>23</sup> The solution was mixed and left for 30 min. To get rid of the excess PAA polymer after coating,

the coated GNR suspension was centrifuged for 10 min at 10,000 rpm, and the pellets were resuspended in purified 18 M $\Omega$  water.

### PAH coating of PAA-GNR

To each 1.0 mL of purified PAA-GNR suspension, 0.2 mL of PAH solution (10 mg/mL prepared in 10 mM NaCl solution) and 0.1 mL NaCl solution (10 mM) were added simultaneously.<sup>23</sup> The solution was mixed and left for 30 min. To get rid of the excess PAH polymer, the coated GNR suspension was centrifuged for 10 min at 10,000 rpm, and the pellets were resuspended in purified 18 M $\Omega$  water.

### PEGylation of GNR (PEG-GNR)

To each 1.0 mL of twice cleaned CTAB-GNR suspension, 0.1 mL of PEG-SH solution (10 mg/mL) was added and mixed for 12 h.<sup>24</sup> To get rid of the excess PEG-SH polymer after coating, the coated GNR suspension was centrifuged twice for 10 min at 10,000 rpm, and the pellets were resuspended in purified 18 M $\Omega$  water.

### Preparation of PEG-cystamine-GNR (PEG-Cys-GNR)

To each 1.0 mL of twice cleaned CTAB-GNR suspension, 0.1 mL of PEG-SH solution (5 mg/mL) were added and mixed for 6 h. To get rid of the excess PEG polymer after coating, the coated GNR suspension was centrifuged for 10 min at 10,000 rpm, and the pellets were resuspended in purified 18 M $\Omega$  water. To each 10 mL of purified PEG-GNR suspension, 1.0 mL of cystamine dihydrochloride (30 mM) was added and mixed overnight. To get rid of the excess cystamine dihydrochloride after coating, the coated GNR solution was centrifuged for 10 min at 10,000 rpm, and the pellets were resuspended in purified 18 M $\Omega$  water.<sup>25</sup>

### Evaluation of colloidal stability of PEG-GNR, PAA-GNR, PAH-GNR, and PEG-Cys-GNR suspensions upon mixing with bacterial growth media

A volume of 100  $\mu$ L (4.0, 2.0, and 1.0 nM) of each PEG-GNR, PAA-GNR, PAH-GNR and PEG-Cys-GNR suspensions was mixed with 100  $\mu$ L of bacterial growth media (Mueller–Hinton broth or reinforced clostridial broth) and incubated either aerobically at 37°C for 24 h in Mueller–Hinton broth or under anaerobic conditions at 37°C for 72 h in reinforced clostridial broth. The color change of the mixtures was observed, and the optical spectra were recorded

to follow aggregation of nanoparticles. All experiments were done in triplicate.

### Assessment of minimum inhibitory concentration (MIC) of GNR suspensions (PEG-GNR, PAA-GNR, and PEG-Cys-GNR) and free ligand solutions (PEG-SH, PAA, and cystamine dihydrochloride) against *S. aureus* and *P. acnes*

Overnight culture of *S. aureus* and 72 h culture grown under anaerobic conditions (15% CO<sub>2</sub>) of *P. acnes* were used in this study. MIC of each GNR suspension (PEG-GNR, PAA-GNR, and PEG-Cys-GNR) was determined against *S. aureus* and *P. acnes* using twofold broth microdilution method in 96-well plates.<sup>26,27</sup> Double-strength medium (100  $\mu$ L) of Mueller–Hinton broth for *S. aureus* or reinforced clostridial broth for *P. acnes* was used to fill the first experimental well. The other wells were filled with single-strength medium (100  $\mu$ L). A volume of 100  $\mu$ L of GNR suspensions (4.0 nM) was added to the first well. Double fold serial dilutions were then carried out across the plate. A volume of 10  $\mu$ L of the cultured microorganisms (*S. aureus* or *P. acnes*) was used to inoculate each well to achieve an inoculum size of ca. 1.5 $\times$ 10<sup>6</sup> CFU/mL. The plates were then incubated aerobically at 37°C for 24 h for *S. aureus* or under anaerobic conditions at 37°C for 72 h for *P. acnes*. MIC was expressed as the mean concentration between the well showing growth (turbidity) and that showing no growth.<sup>27</sup> Negative controls were performed with only sterile broth, and positive controls were performed with only bacterial culture with media in the wells.

MIC of the following ligand solutions: PEG-SH (50 mg/mL), PAA (10 mg/mL), and cystamine dihydrochloride (30 mM) was determined as described earlier. The experiments were done in triplicate.

### Assessment of MIC of supernatants of GNR suspensions and the extra-purified GNR suspensions (GNR 2) against *S. aureus* and *P. acnes*

A certain volume of each prepared GNR suspension (PEG-GNR, PAA-GNR, and PEG-Cys-GNR) was centrifuged at 10,000 rpm for 10 min. The MIC of 100  $\mu$ L of the resultant supernatant of each GNR suspension was measured against *S. aureus* and *P. acnes* using the method described in the “Assessment of MIC of GNR suspensions (PEG-GNR, PAA-GNR, and PEG-Cys-GNR) and free ligand solutions

(PEG-SH, PAA, and cystamine dihydrochloride) against *S. aureus* and *P. acnes*” section.

The resultant pellets after centrifugation of each GNR suspension were reconstituted with ultrapure water to obtain a concentration of 4.0 nM of “an extra-purified GNR” suspension, presented as GNR 2. The MIC of each GNR 2 suspension was measured as described in the “Assessment of MIC of GNR suspensions (PEG-GNR, PAA-GNR, and PEG-Cys-GNR) and free ligand solutions (PEG-SH, PAA, and cystamine dihydrochloride) against *S. aureus* and *P. acnes*” section.

A certain volume of each GNR 2 suspension was centrifuged again, and MIC of the second resultant supernatant, presented as “supernatant 2” (100  $\mu$ L), was measured again against *S. aureus* and *P. acnes*. The MIC values of the supernatants are presented as the concentration of GNR at which its corresponding supernatant caused an effect. The experiments were done in triplicate.

### Assessment of minimum bactericidal concentration (MBC) of GNR suspensions against *S. aureus* and *P. acnes*

The setup of MIC testing described in the “Assessment of MIC of GNR suspensions (PEG-GNR, PAA-GNR, and PEG-Cys-GNR) and free ligand solutions (PEG-SH, PAA, and cystamine dihydrochloride) against *S. aureus* and *P. acnes*” section was used for the determination of the MBC values for GNR suspensions using the standard plate count method.<sup>27,28</sup> From each well showing no turbidity, as well as from the control, a volume of 100  $\mu$ L was transferred to 900  $\mu$ L of normal saline. Tenfold serial dilution was carried out and 100  $\mu$ L of each diluted mixture (five mixtures) were spread onto nutrient agar plates for *S. aureus* or reinforced clostridial agar for *P. acnes* and incubated at 37°C for 24 h for *S. aureus* or under anaerobic condition for *P. acnes*. Neutralization of the antimicrobial activity of the tested compound was achieved by dilution. The MBC value is defined as the lowest concentration showing no growth after incubation. The experiment was done in triplicate.

### SEM imaging of *S. aureus* treated with PEG-GNR

SEM imaging of *S. aureus* treated with PEG-GNR suspension was carried out using poly-L-lysine-coated slide.<sup>29</sup> A volume of 100  $\mu$ L of PEG-GNR suspension (1.25 nM) was mixed with 100  $\mu$ L of Mueller–Hinton broth and 10  $\mu$ L of microorganism (ca.  $1.5 \times 10^6$  CFU/mL) and incubated for

1 h. The mixture was then centrifuged at 15,000 rpm for 20 min, the supernatant was removed, and the pellets were suspended in normal saline. After that, 50  $\mu$ L of the suspension was transferred onto the slide and kept until dry. The sample was then fixed in 3% glutaraldehyde for 3 h and imaged by SEM. SEM imaging of untreated *S. aureus* was performed as a control.

### Statistical analysis

Statistical analysis was performed by applying unpaired *t*-test using GraphPad Prism version 6.0 (San Diego, CA, USA). Results were considered significant when  $p < 0.05$ .

## Results

### Synthesis and characterization of GNR of different surface chemistry

Adopting available protocols, CTAB-GNR, anionic PAA-GNR, cationic PAH-GNR, and neutral PEG-GNR suspensions were successfully synthesized (Figure 1A–C). Another cationic GNR suspension with superior stability was prepared utilizing cystamine hydrochloride and PEG moieties as per reported protocol (Figure 1D).<sup>25</sup> The prepared GNR suspensions were characterized by UV-vis absorption spectroscopy, zeta potential, and TEM imaging. Optical spectra showed typical transverse and longitudinal plasmon peaks of CTAB-GNR (520, 800 nm, respectively) (Figure 2A) with length, width, and aspect ratio of  $\sim 49.5$  nm,  $\sim 12$  nm, and  $\sim 4.2$ , respectively, as confirmed by TEM analysis (Figure 2C). The effective surface charge of CTAB-GNR, PAH-GNR, and PEG-Cys-GNR was cationic (+26, +59, and +55 mV respectively), PAA-GNR were anionic (–72 mV) and PEG-GNR were around neutral (–6 mV) (Figure 2B).

### Colloidal stability of PEG-GNR, PAA-GNR, PAH-GNR, and PEG-Cys-GNR upon mixing with bacterial growth media

The stability results upon mixing of GNR suspensions of different surface chemistry with Mueller–Hinton broth are presented in Figure 3. The color of GNR suspensions and bacterial growth media are deep brown and creamy yellow, respectively. The color of a stable mixture of GNR suspension and growth medium is deep brown. Neutral (PEG-GNR), anionic (PAA-GNR), and cationic (PEG-Cys-GNR) suspensions showed no color change or UV-vis absorption peak broadening, which confirmed their excellent colloidal stability upon mixing with growth medium over 24 h

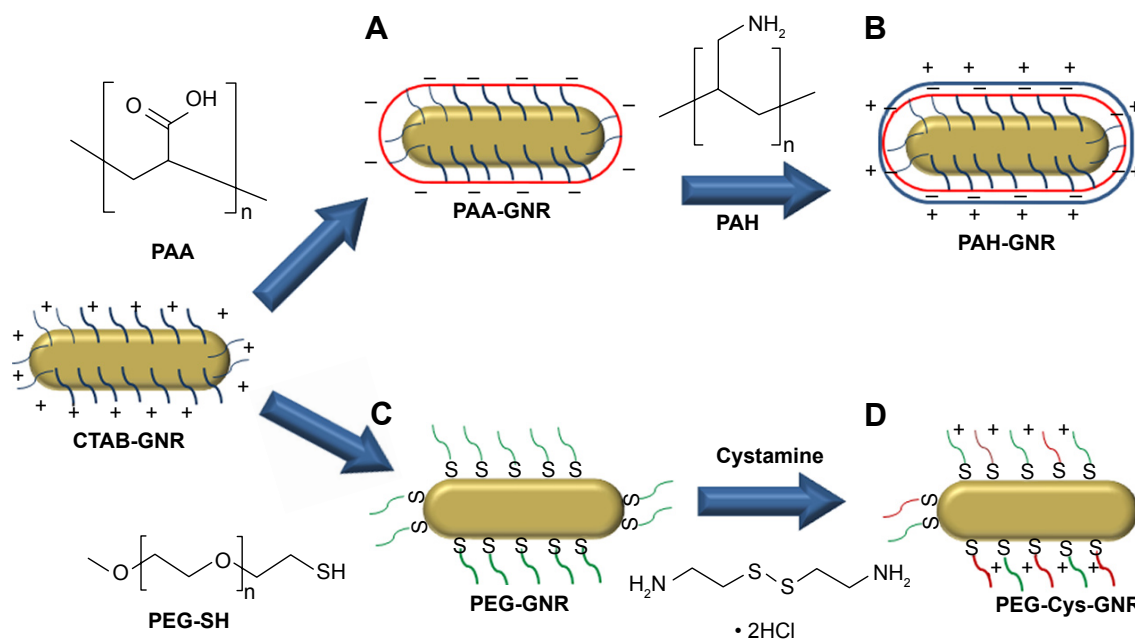


**Figure 1** Functionalization of CTAB-GNR surface with: (A) anionic polyelectrolyte, PAA; (B) cationic polyelectrolyte, PAH; (C) neutral PEG-SH; and (D) PEG-SH followed by cationic cystamine hydrochloride.

**Abbreviations:** CTAB, cetyltrimethylammonium bromide; GNR, gold nanorods; PAA, polyacrylic acid; PAH, polyallylamine hydrochloride; PEG-SH, polyethylene glycol thiol.

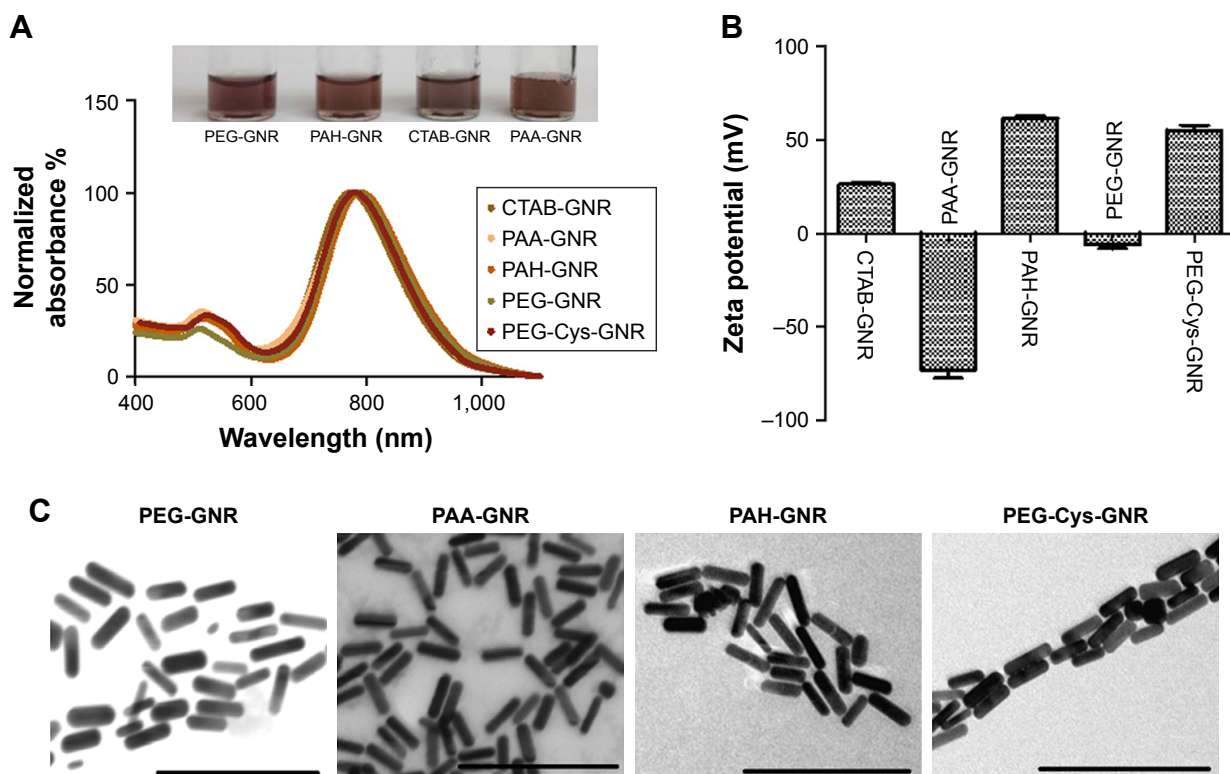


**Figure 2** Characterization of GNR of different surface chemistry as labeled.

**Notes:** (A) UV-vis absorption spectra of GNR suspensions (real picture of GNR vials is shown in the inset). (B) Effective surface charge of GNR functionalized with different ligands. (C) TEM images of GNR of different surface chemistry. Scale bar = 200 nm.

**Abbreviations:** CTAB, cetyltrimethylammonium bromide; GNR, gold nanorods; PAA, polyacrylic acid; PAH, polyallylamine hydrochloride; PEG, polyethylene glycol; TEM, transmission electron microscope; UV-vis, ultraviolet-visible.

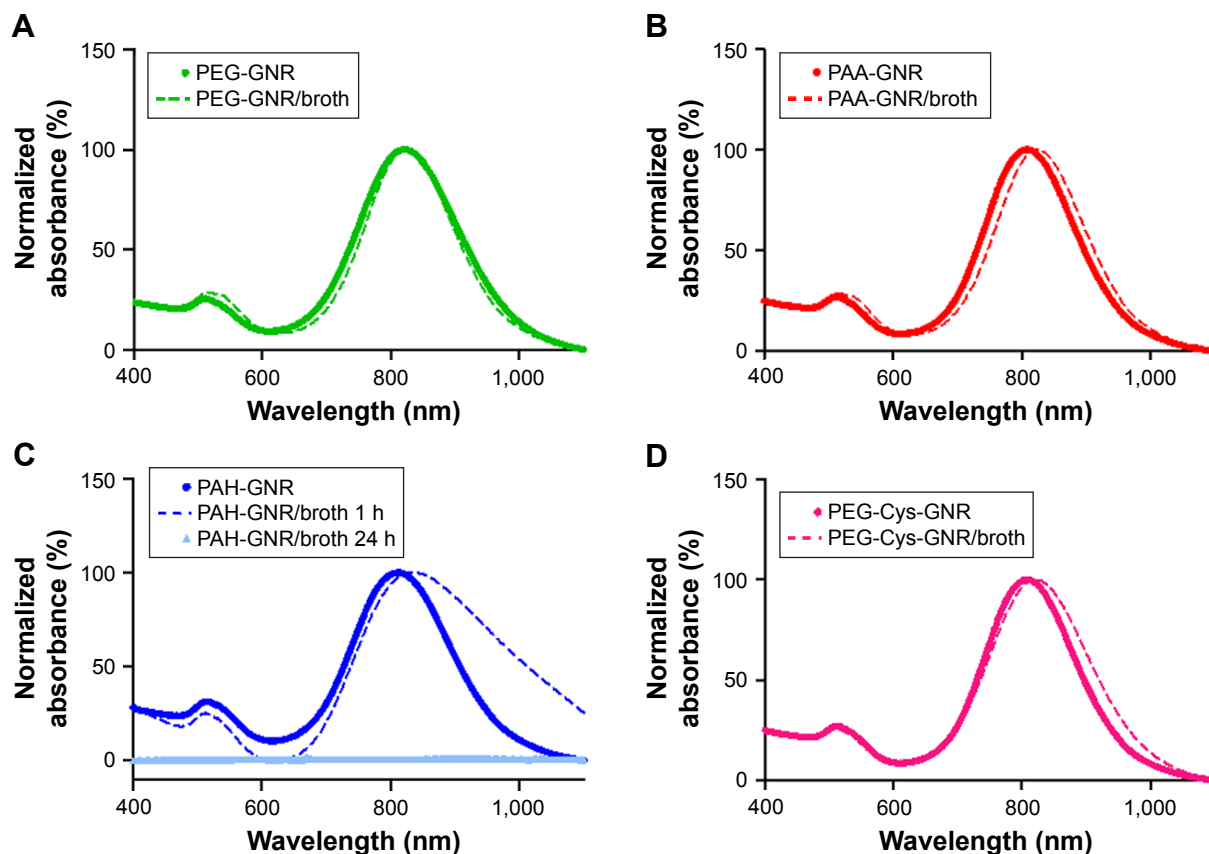


**Figure 3** UV-vis absorption spectra of (A) PEG-GNR, (B) PAA-GNR, (C) PAH-GNR, and (D) PEG-Cys-GNR suspensions before (solid lines) and after (dashed lines) mixing with nutrient growth (Mueller–Hinton broth) over 24 h.

**Abbreviations:** GNR, gold nanorods; PAA, polyacrylic acid; PAH, polyallylamine hydrochloride; PEG, polyethylene glycol; UV-vis, ultraviolet–visible.

(Figure 3A, B, and D). However, PAH-GNR suspension showed color change and UV-vis absorption peak broadening after 1 h of incubation with the growth medium, and a complete aggregation and precipitation out of the suspension after 24 h (Figure 3C).

Figure 4 demonstrates the color of GNR suspensions of different surface chemistry when mixed with Mueller–Hinton broth medium used for *S. aureus*. Cationic PAH-GNR suspension exhibited color change (from brown to blue), which is a typical sign of aggregation of nanoparticles. Similar results (not shown) were obtained upon mixing of the tested GNR suspensions with reinforced clostridial broth medium.

### MIC and MBC of GNR suspensions, their ligands, and supernatant controls against *S. aureus* and *P. acnes*

Since PAH-GNR suspension exhibited severe aggregation upon mixing with bacterial growth media, the antibacterial activity tests were not conducted on them in this study. Instead, the cationic PEG-Cys-GNR suspension which showed excellent colloidal stability was used.

The systematic antibacterial evaluation protocol used in this study is demonstrated in Figure 5.

MIC values of GNR and the extra-purified (GNR 2) suspensions against *S. aureus* and *P. acnes* are presented

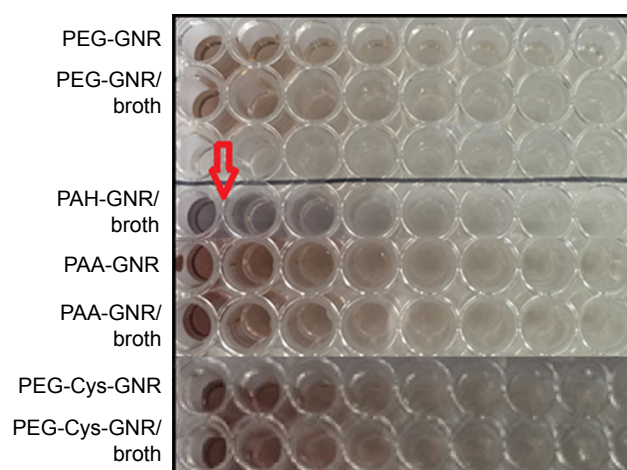


**Figure 4** Color of GNR suspensions of different surface chemistry after mixing with Mueller–Hinton broth for 24 h.

**Note:** The red arrow indicates the color change of PAH-GNR from brown to blue upon mixing with the media.

**Abbreviations:** GNR, gold nanorods; PAA, polyacrylic acid; PAH, polyallylamine hydrochloride; PEG, polyethylene glycol.

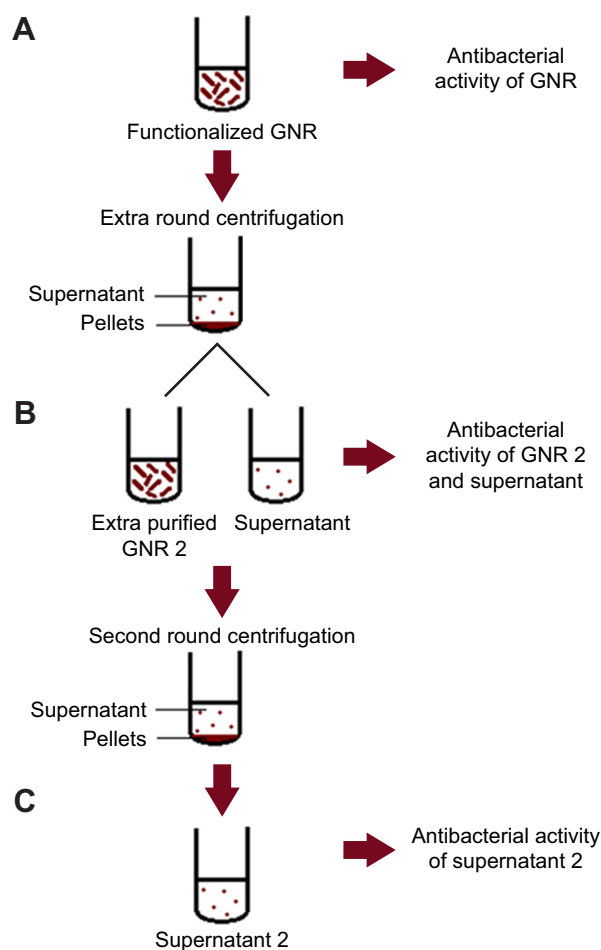


**Figure 5** Cartoon demonstration of the antibacterial activity assessment protocol of GNR suspensions and their corresponding supernatant solutions.

**Notes:** (A) Assessment of antibacterial activity of the original GNR suspension. (B) Assessment of antibacterial activity of the supernatant and the extra-purified GNR suspension (GNR 2). (C) Assessment of antibacterial activity of second supernatants (supernatants 2) of GNR 2 suspension.

**Abbreviation:** GNR, gold nanorods.

in Figure 6, where PEG-GNR and PAA-GNR suspensions exhibited statistically similar MIC values, which are significantly lower than MIC value of PEG-Cys-GNR suspension against *S. aureus* (Figure 6A) and *P. acnes* (Figure 6B). On the other hand, all the ligands used for GNR functionalization (PEG-SH, PAA, and cystamine dihydrochloride) did not show any bacterial growth inhibition over the wide range of concentrations used.

Interestingly, the supernatant of PEG-GNR suspension showed similar antibacterial activity to its original PEG-GNR suspension against *S. aureus*. However, the MIC value of the extra-purified PEG-GNR (PEG-GNR 2) was significantly higher than that of the PEG-GNR (0.461 vs 0.117 nM; Figure 6A). The supernatant of PEG-GNR 2 suspension “ie, supernatant 2” showed no antibacterial activity. Similar results were observed for the anionic PAA-GNR against *S. aureus*, where the MIC of the original PAA-GNR

suspension showed similar antibacterial activity to its corresponding supernatant. However, the MIC value of the extra-purified PAA-GNR (PAA-GNR 2) was significantly higher than that of the original PAA-GNR suspension (0.328 vs 0.082 nM, Figure 6A). On the other hand, the supernatant of cationic PEG-Cys-GNR showed no antibacterial activity against *S. aureus*, and the MIC value of PEG-Cys-GNR is comparable to both MIC values of the extra-purified PEG-GNR 2 and PAA-GNR 2 against *S. aureus* (Figure 6A).

Similar trend of results was observed in the case of *P. acnes* (Figure 6B). Nevertheless, the MIC values of PEG-GNR and PEG-Cys-GNR suspensions were significantly lower against *P. acnes* compared to *S. aureus*. Similarly, the MIC value of PEG-GNR 2 was significantly lower against *P. acnes* compared to *S. aureus* (Figure 6C).

MBC values of GNR suspensions against *S. aureus* (Figure 7A) and *P. acnes* (Figure 7B) were very close to their corresponding MIC values. However, MBC value of PEG-Cys-GNR was much higher than its corresponding MIC value against both *S. aureus* and *P. acnes*.

## Characterization of antibacterial activity of PEG-GNR against *S. aureus* using SEM

Figure 8A presents intact untreated *S. aureus* cocci, while Figure 8B presents *S. aureus* treated with PEG-GNR. The second image reveals the lysis of the bacterial cells upon exposure to PEG-GNR although the GNR did not appear in this image.

## Discussion

CTAB-GNR with aspect ratio (length/width) of ~4 were prepared by wet chemical method where the cationic surfactant (CTAB) was used as a shape-directing agent. CTAB forms a bilayer on the surface of GNR to display the cationic trimethylammonium head groups to the aqueous media. Layer-by-layer (LbL) coating approach was employed to wrap CTAB-GNR with anionic polyelectrolytes resulting in anionic PAA-GNR followed by cationic polyelectrolyte resulting in cationic PAH-GNR (Figure 1A and B). PEGylated GNR were prepared by CTAB displacement on the surface of CTAB-GNR with PEG-SH (Figure 1C). Cationic GNR with superior stability to PAH-GNR were prepared utilizing two moieties: 1) thiolated cationic ligand (cystamine hydrochloride) to provide effective positive surface charge and 2) thiolated PEG-SH to maintain colloidal stability of GNR via steric repulsion (Figure 1D).<sup>18,30</sup> Upon surface functionalization to prepare PAA-GNR and PAH-GNR, no significant broadening or tailing of the

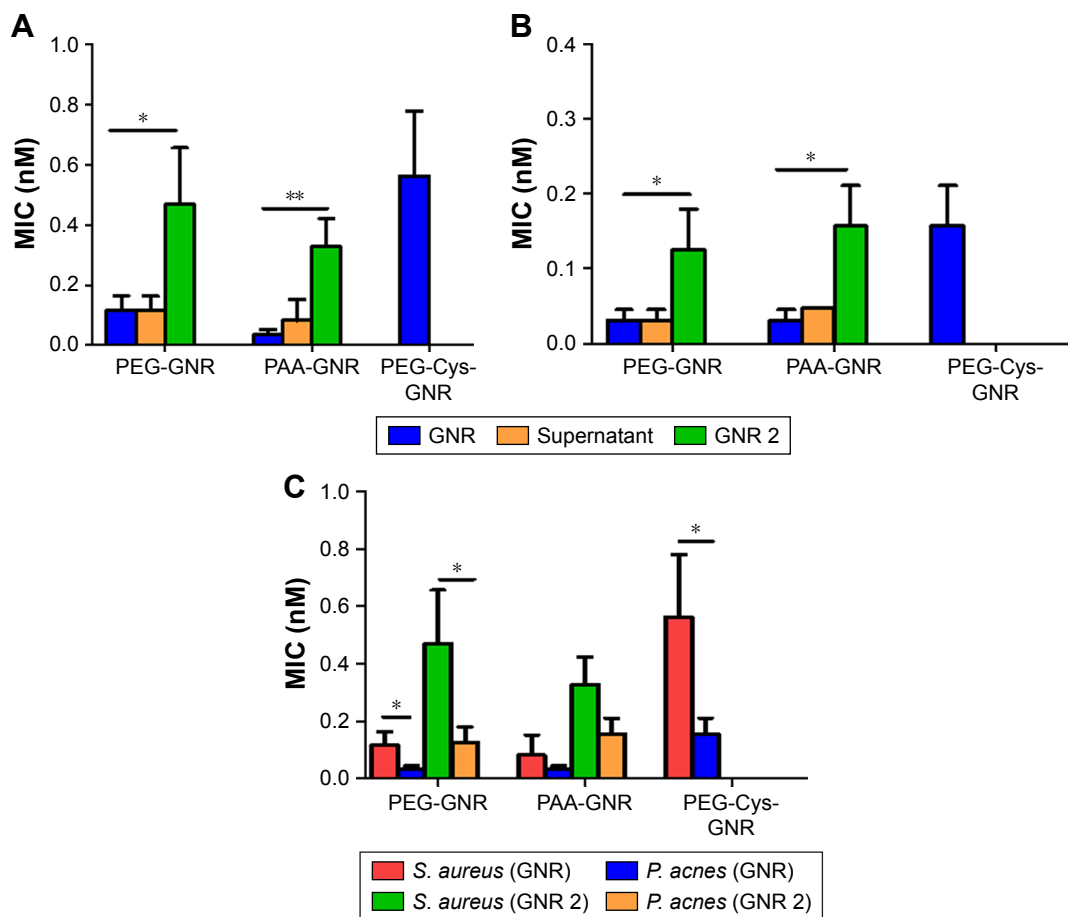


**Figure 6** MIC values of GNR and their supernatants against (A) *Staphylococcus aureus* and (B) *Propionibacterium acnes*. PEG-Cys-GNR supernatant showed no MIC value. (C) MIC values for GNR and GNR 2 against *S. aureus* and *P. acnes*. Notes: MIC values are presented as mean ± SD (n=4). Unpaired t-test was used to evaluate the differences; \*p<0.05. \*\*p<0.01. Abbreviations: GNR, gold nanorod; MIC, minimum inhibitory concentration; PAA, polyacrylic acid; PEG, polyethylene glycol.

longitudinal peaks of the optical spectra was observed, suggesting a maintained colloidal stability without aggregation. The observed small red shift in the longitudinal plasmon peak upon surface modification with (PAA, PAH,

PEG-SH) is attributed to the change in the local refractive index around the GNR core upon surface functionalization (Figure 2A). Furthermore, zeta potential measurement was used to determine and confirm the successful deposition of

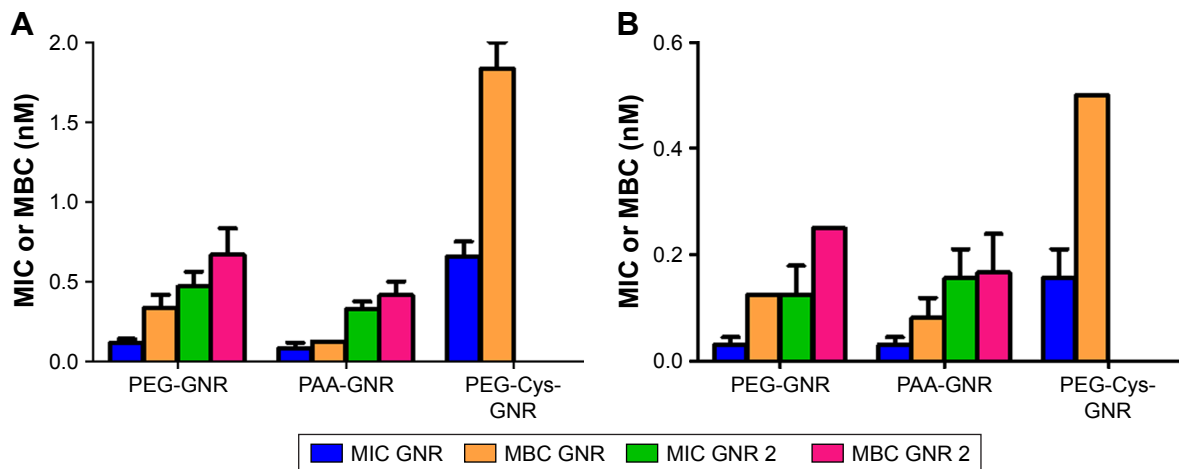


**Figure 7** MIC and MBC values of GNR suspensions of different surface chemistry against (A) *Staphylococcus aureus* and (B) *Propionibacterium acnes*. Abbreviations: GNR, gold nanorods; MBC, minimum bactericidal concentration; MIC, minimum inhibitory concentration; PAA, polyacrylic acid; PEG, polyethylene glycol.



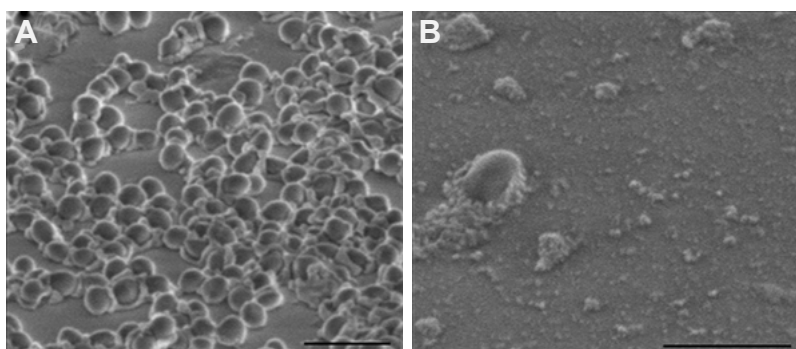


**Figure 8** SEM images of (A) untreated *Staphylococcus aureus* (control) and (B) *S. aureus* treated with PEG-GNR. Scale bars: 2  $\mu\text{m}$ .  
**Abbreviations:** GNR, gold nanorods; SEM, scanning electron microscope; PEG, polyethylene glycol.

ligands onto the nanoparticle surface. For polyelectrolyte coating, effective surface charge reversal after each step of polymer deposition was achieved; the zeta potential of as-prepared GNR (CTAB-GNR) is +26 mV because of the presence of a bilayer of CTAB on the nanorod surface. It can be clearly observed that there is a charge reversal to negative ( $-72$  mV) upon addition of anionic polyelectrolyte polymer (PAA), which confirms adsorption of the anionic polyelectrolyte (due to the ionized carboxylic acid groups) onto oppositely positive charged surfaces (CTAB-GNR) through electrostatic self-assembly. Charge reversal into +59 mV is further utilized for the subsequent adsorption of the cationic polyelectrolyte (PAH) (Figure 2B). On the other hand, the effective surface charge of PEGylated GNR was decreased from +26 to near neutral ( $-6$  mV), which confirms successful displacement of CTAB with PEG-SH by self-assembly (Figure 2B). The slightly negative charge of PEG-GNR may be attributed to adsorption of negatively charged species ( $\text{OH}^-$  or  $\text{PEG-S}^-$ ) on the surface of the particles. The effective surface charge of the nanorods increased from neutral to +55 mV upon addition of cystamine to PEG-GNR in order to provide positive surface charge (Figure 2B). TEM images of GNR functionalized with different ligands are provided in Figure 2C to confirm the size and shape of the nanoparticles.

GNP with non-spherical shape (GNR) were selected for the current study due to their superiority in the photothermal ablation activity, which can be utilized to eliminate bacteria and other microorganisms.

Studying the stability of nanoparticles in biological system is essential as aggregates exert different action/interaction compared to individual nanoparticles.<sup>17,30</sup> Bacterial growth media are generally composed of peptones, which are mixtures of peptides and amino acids obtained by enzymatic digestion or acid hydrolysis of natural products such as animal tissues in addition to the starch and salt. These

components could induce aggregation of nanoparticles. Based on the stability study results, we postulate that adsorption of peptides is the main origin of the observed cationic PAH-GNR aggregation in agreement with our previous study, where we reported that the aggregation of cationic PAH-GNR was strongly correlated with protein adsorption on the surface of GNR by forming a partial corona around them due to their low concentration.<sup>25</sup> Thus, we proposed that the low percentage of peptones in the bacterial growth media (around 2%) provides similar conditions of low protein concentration at which aggregation of nanoparticles is strongly induced. Furthermore, Alkilany et al found that PAH-GNR were stable and were not aggregated after exposure to the cell culture media that contain high percentage of proteins (around 10%), and they proved that the adsorption of proteins on the surface of GNR forming complete corona is responsible for the stabilization of the nanoparticles instead of aggregation,<sup>31</sup> which strongly supports our previous hypothesis of aggregation. On the other hand, the excellent stability of PEG-GNR and PEG-Cys-GNR suspensions upon mixing with bacterial growth media might be related to the presence of PEG shell that provides steric stabilization and prevents non-specific protein adsorption.<sup>18,30</sup> In addition, the excellent stability of the anionic PAA-GNR suspension might be due to the repulsion forces between the negatively charged nanoparticles and peptones in the growth media. Unfortunately, this crucial factor of media-induced aggregation is ignored in the literature and might contribute to the observed conflicting findings.

In microbiology, MIC and MBC values are the most important tests used to evaluate the antibacterial activity of any agent. The MIC is the lowest concentration of an agent that prevents visible growth of a bacterium (at which it has bacteriostatic activity), whereas the MBC is the concentration that results in microbial death (at which it is bactericidal).<sup>26,28</sup>

MIC and MBC results confirmed that GNR pose bacteriostatic and bactericidal activities against *S. aureus* and *P. acnes*. Nevertheless, the role of CTAB, which is a well-known cationic surfactant used in the synthesis of GNR as a shape-directing agent and has a well-documented antibacterial activity,<sup>32,33</sup> cannot be ignored. Accordingly, in addition to GNR intrinsic toxicity, other factors such as impurities and trace ions present in the GNR suspension might highly contribute to the measured activity and lead to misinterpretation of the results. In order to avoid such serious artifacts, the antibacterial activity of GNR corresponding “supernatants”, extra-cleaned GNR suspensions, and ligands used for GNR functionalization was measured in addition to the original GNR suspensions to exclude any possible antibacterial activity that may originate from free molecules in GNR suspensions (such as CTAB) rather than GNR themselves.

The results of the antibacterial activity of GNR suspensions and their supernatants suggest that free CTAB present in the supernatant solutions of GNR suspensions of different surface chemistry might contribute to the observed antibacterial activity, since the antibacterial activity of the colorless supernatant solutions was nearly identical to that of its original deep brown-colored GNR suspension (Figure 6A and B). Moreover, the extra-purified (GNR 2) suspensions have significantly higher MIC values compared to their original GNR suspensions due to decreased CTAB concentration in the suspensions after extra centrifugation. In addition, the extra-purified GNR 2 suspensions have undergone another round of centrifugation and their corresponding supernatants “supernatants 2” showed no antibacterial activity, which strongly supports the role of CTAB in the observed antibacterial activity of GNR (Figure 6A and B).

In addition to the possible contribution of CTAB molecules, the colorless supernatant solutions may also contain leftover gold ions that could contribute to the antibacterial activity. A recent study reported the antibacterial activity of Au(I) and Au(III) toward four different bacteria including *S. aureus*.<sup>34</sup> However, the possible contribution of these ions to the current antibacterial activity of GNR should be minimal compared to the effect of CTAB. In contrast to the GNR suspensions, the supernatant from gold nanosphere suspension (which does not contain CTAB) does not show any antibacterial activity compared to its original nanosphere suspension (data not shown), which supports the high contribution of CTAB to the current observed antibacterial activity of GNR suspensions. In agreement with our results, Alkilany et al reported the contribution of free CTAB molecules, in GNR suspension, for the toxicity of GNR on

cancer culture cells. In addition, they found that gold and silver ion concentrations in the supernatants of GNR were below the detection limits of the instrument used for concentration measurement (inductively coupled plasma with atomic emission spectroscopy), and they were nontoxic.<sup>31</sup>

It is worth to mention here that PEG-Cys-GNR suspension has already undergone two rounds of centrifugations during functionalization process and before antibacterial testing; one after PEGylation and another round after cystamine addition, while other functionalized GNR suspensions have undergone only one round of centrifugation after functionalization and before antibacterial testing. This explains the absence of significant difference of MIC value between PEG-Cys-GNR and the extra-purified suspensions (PEG-GNR 2 and PAA-GNR 2), and the lack of antimicrobial activity of the supernatant of PEG-Cys-GNR compared to the supernatants of PEG-GNR and PAA-GNR suspensions. It is very important to point out here that GNR pellets collected after the second extra-centrifugation round were aggregated and could not be evaluated for their antibacterial activity.

To the best of our knowledge, the antibacterial activity of GNR supernatant was not discussed previously in any of the studies that explored the antibacterial activity of GNR prepared using CTAB. However, we cannot exclude other hypotheses which support that GNR may pose intrinsic antibacterial activity, since the extra-centrifuged GNR suspensions (GNR 2) still exhibited a considerable antibacterial activity although their MIC values were significantly higher than that of original GNR suspensions. In a recent study, the MIC value of non-functionalized GNR (CTAB-GNR) using 0.2 M CTAB was  $\sim 6.5 \mu\text{g/mL}$  against *S. aureus*,<sup>35</sup> which is lower than MIC values of GNR suspensions against *S. aureus* reported in the current study. These results support our hypothesis of CTAB contribution to the observed antibacterial activity since the concentration of CTAB in the non-functionalized GNR is much higher than that of functionalized GNR. Similarly, in another study, the MIC value of non-functionalized GNR (CTAB-GNR) was  $\sim 15.6 \mu\text{g/mL}$  against *S. aureus*,<sup>36</sup> which is in the range of the currently reported MIC values of GNR suspensions against *S. aureus*. In the previous studies and other similar studies, neither the colloidal stability of GNR nor the supernatant control was investigated, which are two factors that might have a significant effect on the reported antibacterial activity due to the extent of interface contact and CTAB effect, respectively.

Moreover, MBC values of PEG-GNR and PEG-GNR 2, PAA-GNR and PAA-GNR 2 were very close to their corresponding MIC values, which suggests the bactericidal effect of GNR which is mainly related to the presence of

CTAB and might be related also to the GNR themselves (Figure 7A and B).

Other factor that might affect the reported antibacterial activity of the GNR is their surface chemistry; nevertheless, the reported results are conflicting. In a recent study, authors reported that negatively charged GNP cannot inhibit *Pseudomonas aeruginosa* compared to the positively charged GNP,<sup>37</sup> while the bacterial activity of positively charged GNP was higher than the negatively charged counterparts in another study.<sup>38</sup> Our results indicated that the MIC value of the anionic PAA-GNR is not significantly different than that for neutral PEG-GNR, and the MIC value of PAA-GNR 2 is not significantly different than that for cationic PEG-Cys-GNR or neutral PEG-GNR 2 against *S. aureus* and *P. acnes*. In another study, cationic and hydrophobic nanoparticles have demonstrated growth suppression of both Gram-positive and Gram-negative bacteria.<sup>9</sup> However, some reports in the literature indicate that the degree of surface negativity and hydrophobicity of Gram-positive bacteria is not the same for all species and strains. For example, Rawlinson et al, found that cationic antimicrobial polymer is more active against *S. epidermidis* than *S. aureus* due to decreased hydrophobicity and increased negative surface charge on *S. epidermidis* compared to *S. aureus*. In addition, they demonstrated that *S. aureus* might develop resistance toward cationic antimicrobial agents due to modification in the peptidoglycan.<sup>39</sup>

Furthermore, capping GNR with PEG reduces the tendency of particles to aggregate and increases their compatibility with biological media because it decreases the non-specific protein adsorption.<sup>40</sup> Based on these properties of PEG-GNR, and in addition to their unique hydrophobicity/hydrophilicity characteristics, we propose that PEGylation of GNR may enhance the penetration of PEG-GNR into the biological matrices with considerable stability and subsequently improve their uptake by bacteria. Nevertheless, the conflicting results in the published studies might be due to inconsistency in purification and thus the possible contribution of CTAB as an overlooked artifact.

The results of SEM imaging are in good agreement with the reported bactericidal activity of the tested GNR suspensions. Reported MBC values indicated the effectiveness of GNR in eradicating the *S. aureus*, which is most likely related to the presence of CTAB in GNR solutions.

Overall, the abovementioned results strongly suggest that the documented antibacterial activity of GNR in the literature might be an artifact due to the possible contribution of CTAB to the observed antibacterial activity. Accordingly, the proper design of controls in the experiments is crucial to

avoid misinterpretation of results and findings. Nevertheless, we cannot exclude the intrinsic toxicity of GNR and the effect of their surface chemistry.

Furthermore, this study demonstrated that the standard growth media commonly used in the assessment of antimicrobial activities is not always suitable to be used since it might destabilize certain types of GNP, which needs further studies to design specific modified media for such nanoparticles.

## Conclusion

GNR are promising candidates for eradication of *S. aureus* and *P. acnes* that are responsible for skin and follicular diseases such as acne vulgaris. However, the colloidal stability of GNR suspensions upon mixing with growth media should be evaluated first since the aggregated particles will behave differently when exposed to cells or bacteria. In addition, the contribution of CTAB to the observed antibacterial activity highlighted the importance of the proper design of controls to prevent misinterpretation of the outcomes. Nevertheless, the antibacterial activity of GNRs by themselves could not be excluded and it needs further studies to elaborate the possible mechanisms responsible for their activity.

## Acknowledgments

The authors thank the Deanship of Academic research and Quality Assurance, the University of Jordan (grant number: 152/2014-2015) for financial support. Current address for NNM: Department of Pharmacy, Faculty of Pharmacy, Al-Zaytoonah University of Jordan, Amman 11733, Jordan.

## Disclosure

The authors report no conflicts of interest in this work.

## References

1. Jain PK, Huang X, El-Sayed IH, El-Sayed MA. Noble metals on the nanoscale: optical and photothermal properties and some applications in imaging, sensing, biology, and medicine. *Acc Chem Res.* 2008;41(12):1578–1586.
2. Allahverdiyev AM, Kon KV, Abamor ES, Bagirova M, Rafailovich M. Coping with antibiotic resistance: combining nanoparticles with antibiotics and other antimicrobial agents. *Expert Rev Anti Infect Ther.* 2011;9(11):1035–1052.
3. Dykman VP, Khlebtsov N. Gold nanoparticles in biomedical applications: recent advances and perspectives. *Chem Soc Rev.* 2012;41(6):2256–2282.
4. Norman RS, Stone JW, Gole A, Murphy CJ, Sabo-Attwood TL. Targeted photothermal lysis of the pathogenic bacteria, *Pseudomonas aeruginosa*, with gold nanorods. *Nano Lett.* 2008;8(1):302–306.
5. Zharov VP, Mercer KE, Galitovskaya EN, Smeltzer MS. Photothermal nanotherapeutics and nanodiagnostics for selective killing of bacteria targeted with gold nanoparticles. *Biophys J.* 2006;90(2):619–627.
6. Amin RM, Mohamed MB, Ramadan MA, Verwanger T, Krammer B. Rapid and sensitive microplate assay for screening the effect of silver and gold nanoparticles on bacteria. *Nanomedicine.* 2009;4(6):637–643.

7. Chatterjee S, Bandyopadhyay A, Sarkar K. Effect of iron oxide and gold nanoparticles on bacterial growth leading towards biological application. *J Nanobiotechnology*. 2011;9:34.
8. Kuo YL, Wang SG, Wu CY, et al. Functional gold nanoparticle-based antibacterial agents for nosocomial and antibiotic-resistant bacteria. *Nanomedicine*. 2016;11(19):2497–2510.
9. Li X, Robinson SM, Gupta A, et al. Functional gold nanoparticles as potent antimicrobial agents against multi-drug-resistant bacteria. *ACS Nano*. 2014;8(10):10682–10686.
10. Penders J, Stolzoff M, Hickey DJ, Andersson M, Webster TJ. Shape-dependent antibacterial effects of non-cytotoxic gold nanoparticles. *Int J Nanomedicine*. 2017;29:2457–2468.
11. Zhou Y, Kong Y, Kundu S, Cirillo JD, Liang H. Antibacterial activities of gold and silver nanoparticles against *Escherichia coli* and bacillus Calmette-Guerin. *J Nanobiotechnology*. 2012;10:19.
12. Webster GF. The pathophysiology of acne. *Cutis*. 2005;76:4–7.
13. Burkhart CN, Gottwald L. Assessment of etiologic agents in acne pathogenesis. *Skinmed*. 2003;2(4):222–228.
14. Fernandes R, Smyth NR, Muskens OL, et al. Interactions of skin with gold nanoparticles of different surface charge, shape, and functionality. *Small*. 2015;11(6):713–721.
15. Mahmoud NN, Alkilany AM, Dietrich D, Karst U, Al-Bakri AG, Khalil EA. Preferential accumulation of gold nanorods into human skin hair follicles: effect of nanoparticle surface chemistry. *J Colloid Interface Sci*. 2017;503:95–102.
16. Lee O, Jeong SH, Shin WU, Lee G, Oh C, Son SW. Influence of surface charge of goldnanorods on skin penetration. *Skin Res Technol*. 2013;19(1):e390–e396.
17. Rausch K, Reuter A, Fischer K, Schmidt M. Evaluation of nanoparticle aggregation in human blood serum. *Biomacromolecules*. 2010;11(11):2836–2839.
18. Urban DA, Rodriguez-Lorenzo L, Balog S, Kinnear C, Rothen-Rutishauser B, Petri-Fink A. Plasmonic nanoparticles and their characterization in physiological fluids. *Colloids Surf B Biointerfaces*. 2016;137:39–49.
19. Beddow J, Stolpe B, Cole P, et al. Effects of engineered silver nanoparticles on the growth and activity of ecologically important microbes. *Environ Microbiol Rep*. 2014;6(5):448–458.
20. Römer I, White TA, Baalousha M, Chipman K, Viant MR, Lead JR. Aggregation and dispersion of silver nanoparticles in exposure media for aquatic toxicity tests. *J Chromatogr A*. 2011;1218(27):4226–4233.
21. Pelletier DA, Suresh AK, Holton GA, et al. Effects of engineered cerium oxide nanoparticles on bacterial growth and viability. *Appl Environ Microbiol*. 2010;76(24):7981–7989.
22. Sau TK, Murphy CJ. Seeded high yield synthesis of short Au nanorods in aqueous solution. *Langmuir*. 2004;20(15):6414–6420.
23. Gole A, Murphy CJ. Polyelectrolyte-coated gold nanorods: synthesis, characterization and immobilization. *Chem Mater*. 2005;17:1325–1330.
24. Alkilany AM, Abulatefeh SR, Mills KK, et al. Colloidal stability of citrate and mercaptoacetic acid capped gold nanoparticles upon lyophilization: effect of capping ligand attachment and type of cryoprotectants. *Langmuir*. 2014;30(46):13799–13808.
25. Mahmoud NN, Al-Qaoud KM, Al-Bakri AG, Alkilany AM, Khalil EA. Colloidal stability of gold nanorod solution upon exposure to excised human skin: effect of surface chemistry and protein adsorption. *Int J Biochem Cell Biol*. 2016;75:223–231.
26. The Clinical and Laboratory Standards Institute for antimicrobial susceptibility testing (CLSI). Wayne; 2016.
27. Al-Bakri AG, Othman G, Bustanji Y. The assessment of the antibacterial and antifungal activities of aspirin, EDTA and aspirin-EDTA combination and their effectiveness as antibiofilm agents. *J Appl Microbiol*. 2009;107(1):280–286.
28. M26-A. *Methods for Determining Bactericidal Activity of Antimicrobial Agents; Approved Guideline*. PA: USA; 1999.
29. Fischer ER, Hansen BT, Nair V, Hoyt FH, Dorward DW. Scanning electron microscopy. *Curr Protoc Microbiol*. 2012;Chapter 2:Unit2B.2.
30. Moore TL, Rodriguez-Lorenzo L, Hirsch V, et al. Nanoparticle colloidal stability in cell culture media and impact on cellular interactions. *Chem Soc Rev*. 2015;44(17):6287–6305.
31. Alkilany AM, Nagaria PK, Hexel CR, Shaw TJ, Murphy CJ, Wyatt MD. Cellular uptake and cytotoxicity of gold nanorods: molecular origin of cytotoxicity and surface effects. *Small*. 2009;5(6):701–708.
32. Nakata K, Tsuchido T, Matsumura Y. Antimicrobial cationic surfactant, cetyltrimethylammonium bromide, induces superoxide stress in *Escherichia coli* cells. *J Appl Microbiol*. 2011;110(2):568–579.
33. Russell AD. Factors influencing the efficacy of antimicrobial agents. In: Russell AD, Hugo WB, Ayliffe GAJ, editors. *Principles and Practice of Disinfection, Preservation and Sterilization*. 2nd ed. Oxford: Blackwell Science Publications; 1992:90–92.
34. Shareena Dasari TP, Zhang Y, Yu H. Antibacterial activity and cytotoxicity of gold (I) and (III) ions and gold nanoparticles. *Biochem Pharmacol (Los Angel)*. 2015;4:199.
35. Castillo-Martínez J, Martínez-Castañón G, Martínez-Gutiérrez F, Zavala-Alonso NV, Patiño-Marín N. Antibacterial and antibiofilm activities of the photothermal therapy using gold nanorods against seven different bacterial strains. *J Nanomater*. 2015;2015:7. Article ID 783671.
36. Salouti M, Heidari Z, Ahangari A, Zare S. Enhanced delivery of gentamicin to infection foci due to *Staphylococcus aureus* using gold nanorods. *Drug Deliv*. 2016;23(1):49–54.
37. Zhao Y, Tian Y, Cui Y, Liu W, Ma W, Jiang X. Small molecule-capped gold nanoparticles as potent antibacterial agents that target Gram-negative bacteria. *J Am Chem Soc*. 2010;132(35):12349–12356.
38. Vaara M. Agents that increase the permeability of the outer membrane. *Microbiol Rev*. 1992;56(3):395–411.
39. Rawlinson LA, O’Gara JP, Jones DS, Brayden DJ. Resistance of *Staphylococcus aureus* to the cationic antimicrobial agent poly(2-(dimethylamino ethyl)methacrylate) (pDMAEMA) is influenced by cell-surface charge and hydrophobicity. *J Med Microbiol*. 2011;60(pt 7):968–976.
40. Manson J, Kumar D, Meenan B, Dixon D. Polyethylene glycol functionalized gold nanoparticles: the influence of capping density on stability in various media. *Gold Bull*. 2011;44:99–105.

## International Journal of Nanomedicine

### Publish your work in this journal

The International Journal of Nanomedicine is an international, peer-reviewed journal focusing on the application of nanotechnology in diagnostics, therapeutics, and drug delivery systems throughout the biomedical field. This journal is indexed on PubMed Central, MedLine, CAS, SciSearch®, Current Contents®/Clinical Medicine,

Submit your manuscript here: <http://www.dovepress.com/international-journal-of-nanomedicine-journal>

Dovepress

Journal Citation Reports/Science Edition, EMBASE, Scopus and the Elsevier Bibliographic databases. The manuscript management system is completely online and includes a very quick and fair peer-review system, which is all easy to use. Visit <http://www.dovepress.com/testimonials.php> to read real quotes from published authors.